Given a bimodal distribution with 500 bubbles of 0.5 mm diameter and 1 bubble 10 mm in diameter, the Sauter mean diameter is 4.7 mm (using Equation (V-5)). However, given 500 bubbles of 1 mm in diameter and 1 bubble 10 mm in diameter, the Sauter mean diameter is 2.5 mm. These results show that for a distribution containing smaller bubbles (0.5 mm), the Sauter mean bubble diameter is significently greater than the distribution containing larger bubbles (1 mm), i.e. 4.7 mm for the former versus 2.5 mm for the latter. The obvious problem is the presence of the one large (10 mm) bubble in each of the distributions. If 100,000 small bubbles were sized instead of 500, only then does the value of d_s approaches 0.5 mm for the first case and 1.0 mm for the second. For the molten wax - nitrogen system the problem is further aggravated because of the large number of fine bubbles present in the dispersion, whereas only a few large bubbles are visible. Therefore, by counting only a relatively small number of these fine bubbles the calculated values for the Sauter mean diameter will be larger than the actual values. The margin of this type of error can be reduced by increasing the bubble count (by analyzing more than one photograph per condition). However, this is an arduous task.

D.3. Bubble Size Distribution Using the Dynamic Gas Disengagement Method

Bubble size measurements were made using the dynamic gas disengagement technique (DGD) developed by Sriram and Mann (1977). Experiments were conducted in the 0.051 m ID and the 0.229 m ID glass columns in order to study the effect of operating temperature (200 and 265°C), distributor type, column diameter, and wax type. Majority of the experiments were conducted in the 0.051 m ID column using FT-300 wax, and reactor waxes

(Sasol's Arge reactor wax and Mobil's reactor wax). A few measurements were made in the 0.229 m ID column with FT-300 wax. The 1.85 mm and 4 mm orifice plate, and the 40 μm SMP distributors were used in the small column, while the 19 X 1.85 mm perforated plate distributor was used in the 0.229 m ID column.

The major highlights of these investigations are:

- 1.85 and 4 mm orifice plate distributors gave similar values for d_s with FT-300 wax, while measurements could not be made with the 40μm SMP distributor due to excessive foaming.
- Column diameter did not have a significant effect on the d_s value for FT-300 wax.
- The presence of foam had a strong effect on d_s values. At 265°C the Sauter mean diameter for FT-300 wax was approximately 0.5 mm, irrespective of the amount of foam (or hold-up). However, results from the DGD method obtained in the presence of foam should be interpreted with caution.
- Temperature had a significant effect on the Sauter mean bubble diameter (d_s), with values at 200°C being significantly larger than values at 265°C for all wax types, despite relatively small differences between hold-up values at the two temperatures.
- Distributor type (SMP and 1.85 mm orifice plate) did not have a significant effect on d_s for reactor waxes, however, values with the SMP distributor were consistently lower than those with the 1.85 mm orifice plate distributor.
- Wax type had a significant effect on d_s values, with the smallest bubbles being produced by FT-300 wax and the largest by Mobil reactor

wax. The trends were similar at both 200°C and at 265°C. At 265°C Sauter mean diameters for FT-300 wax were around 0.8 mm for superficial gas velocities greater than 0.05 m/s; while those for Sasol reactor wax approached 2 mm and Mobil reactor wax gave values around 4 to 5 mm.

D.3a. Theory

Sriram and Mann (1977) developed the dynamic gas disengagement (DGD) technique for obtaining the bubble rise velocity and the bubble size distribution in bubble columns. This technique requires the knowledge of the change in liquid level as a function of time, once the gas flow to the bubble column is shut off.

Sriram and Mann showed that the gas hold-up, $\epsilon_g(t)$, after a time, t, is given by

$$\epsilon_g(t) = \epsilon_{go} \int_0^\infty \left\{ f(d_B) \left[1 - \frac{tu(d_B)}{H(t)} \right] \right\} d(d_B) \qquad (V\text{-}6)$$

where $(1-tu(d_B)/H(t))$ is the fraction of the volume fraction of bubbles remaining in the dispersion after an elapsed time, t. ϵ_{go} is the average gas hold-up at time zero, $f(d_B)d(d_B)$ is the volume fraction of the bubbles having size between d_B and $d_B + d(d_B)$, and $u(d_B)$ is the rise velocity associated with a bubble of size d_B. Equation (V-6), based on a theoretical approach, implies that the bubble size distribution is initially axially homogeneous and that significant bubble interactions do not occur during the disengagement process.

D.3a.1. Discretization for N Classes of Bubbles

A generalized theory for obtaining the bubble size distribution from DGD is developed here. Equations for the specific cases involving bimodal

and trimodal distributions (most commonly encountered in the present work) are presented in APPENDIX C, together with examples and sample calculations. Equation (V-6) is valid for a continuous bubble size distribution, and its discretized version for N classes of bubbles is given by

$$\epsilon_g(t) = \epsilon_{go} \sum_{i=1}^{N} f_i \left[1 - \frac{tu_{Bi}}{H} \right] \qquad \text{(V-7)}$$

where i represents the individual bubble classes, f_i is the volume fraction of bubbles in class i, and u_{Bi} is the rise velocity associated with this class of bubbles. It is assumed that class N comprises of the largest bubbles and class 1 contains the smallest bubbles.

After a time, t_1^*, all of the bubbles in class N will have disengaged along with some bubbles in the other N-1 classes. Similarly, after a time t_2^* ($t_2^* > t_1^*$) all of the bubbles in class N-1 will have disengaged, and so on (see Figure V-64). By this assumption, the term $(1-tu_{BN}/H)$ becomes zero at time t_1^*, the term $(1-tu_{BN-1}/H)$ becomes zero at time t_2^*, leading to the following general equation for the dynamic hold-up, $\epsilon_g(t)$:

$$\epsilon_g(t) = \epsilon_{go} \sum_{i=1}^{k} f_i \left[1 - \frac{tu_{Bi}}{H} \right] \qquad t_{N-k+1}^* \geq t > t_{N-k}^* \qquad \text{(V-8)}$$

Equation (V-8) can be rearranged so as to relate the normalized liquid level (H/H_o) to time elapsed (t) to obtain the following equation (see APPENDIX C for details of its derivation):

$$\frac{H}{H_o} = \frac{H_s/H_o}{1 - \sum_{i=1}^{k} \epsilon_{goi}} - t \frac{\sum_{i=1}^{k} \epsilon_{goi} u_{Bi}}{H_o \left[1 - \sum_{i=1}^{k} \epsilon_{goi} \right]} \qquad t_{N-k+1}^* \geq t > t_{N-k}^* \qquad \text{(V-9)}$$

where $\epsilon_{goi} = \epsilon_{go} f_i$, and H_s is the height of the ungassed liquid (or static height).

According to Equation (V-9) a plot of the normalized liquid level (H/H_o) versus time elapsed (t) would result in a series of straight lines, one for each of the time intervals, with intersections (or break points) occurring at times t_1^*, t_2^*, and so on. This is graphically illustrated in Figure V-64.

D.3a.2. Procedure for Obtaining ϵ_{goi}, u_{Bi} and f_i

Assuming that the experimental normalized liquid level versus time elapsed data can be represented by N straight lines, as shown in Figure V-64, the following procedure can be used to obtain estimates for ϵ_{goi} and u_{Bi}. In Figure V-64, t_N^* represents the time when all bubbles have disengaged from the liquid, therefore, the straight line beyond t_N^* represents the static liquid level. The slope of this line is zero (s_o=0) and the intercept is H_s/H_o (i.e. $b_o = H_s/H_o$).

The first step is to obtain the slopes and intercepts of the N straight line segments (see Figure V-64). Let s_1 to s_N represent the slopes of these lines, and let b_1 to b_N represent the intercepts of these lines. Equation (V-9) can be used to obtain the expressions for the slope and intercept of the straight lines. General equations for estimating ϵ_{goi} and u_{Bi} from s_i and b_i are developed here.

For the k'th straight line the following expressions represent the slope and the intercept:

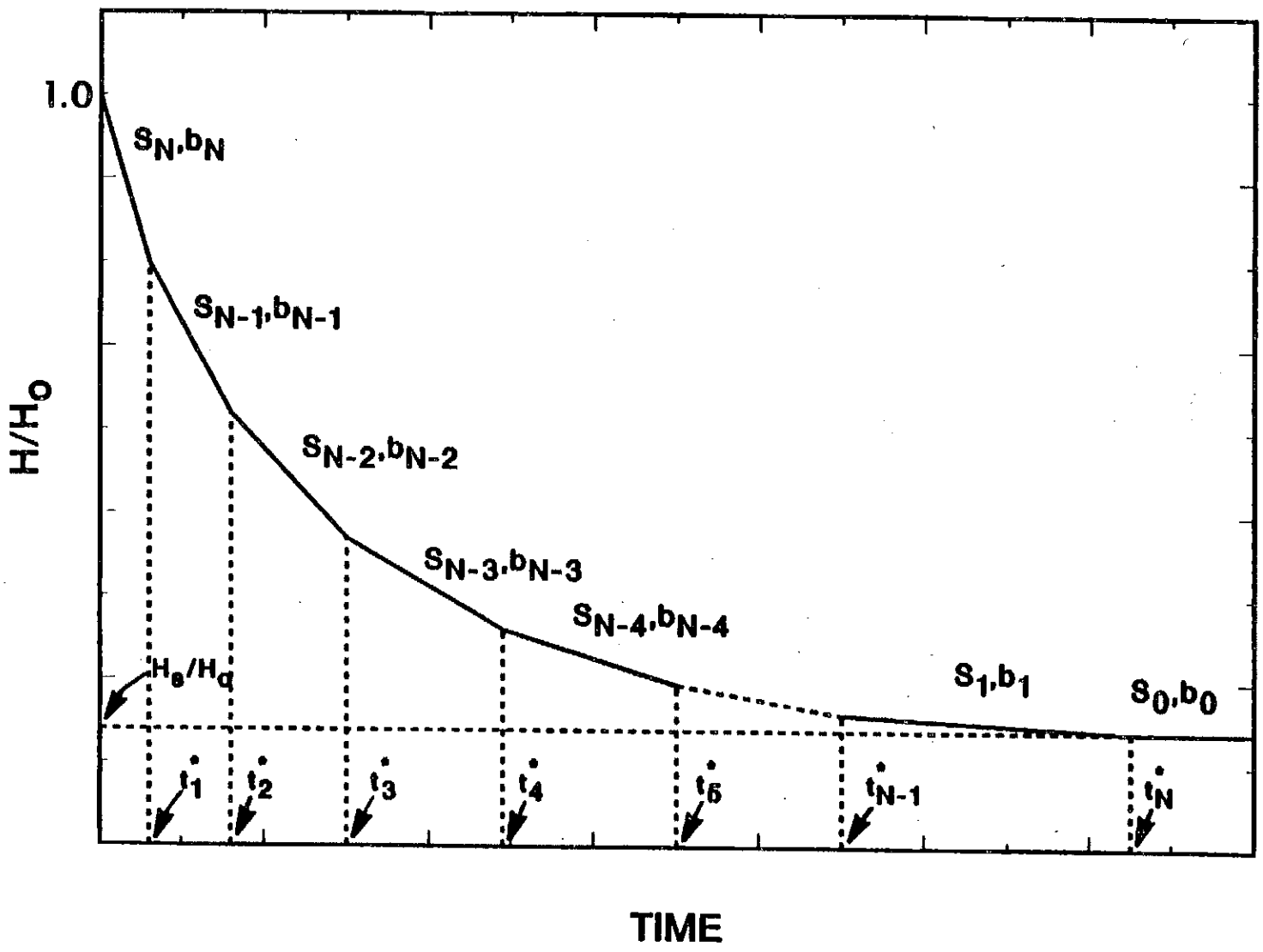

Figure V-64. Change in normalized liquid level with time during DGD for a dispersion with N bubble size classes

$$\text{slope:} \qquad s_k = - \frac{\sum_{i=1}^{k} \epsilon_{goi} u_{Bi}}{H_o \left[1 - \sum_{i=1}^{k} \epsilon_{goi} \right]} \qquad \text{(V-10)}$$

$$\text{intercept:} \qquad b_k = \frac{H_s/H_o}{1 - \sum_{i=1}^{k} \epsilon_{goi}} \qquad \text{(V-11)}$$

These equations can be manipulated to obtain the following expressions for ϵ_{goi} and u_{Bi} (see APPENDIX C for details).

$$\epsilon_{goi} = \frac{H_s}{H_o} \left[\frac{1}{b_{i-1}} - \frac{1}{b_i} \right] \qquad i = 1 \rightarrow N \qquad \text{(V-12)}$$

$$u_{Bi} = \frac{H_o \left[b_i s_{i-1} - b_{i-1} s_i \right]}{b_i - b_{i-1}} \qquad i = 1 \rightarrow N \qquad \text{(V-13)}$$

Equations (V-12) and (V-13) can now be used to estimate ϵ_{goi} and u_{Bi} for the N classes of bubble sizes. The fraction of bubbles in class i, f_i, is given as:

$$f_i = \frac{\epsilon_{goi}}{\epsilon_{go}} \qquad i = 1 \rightarrow N \qquad \text{(V-14)}$$

D.3a.3. Procedure for Obtaining Bubble Size (d_{Bi}) and Number of Bubbles (n_i)

There are several correlations available in literature for obtaining bubble sizes based on the bubble rise velocity. Two of these correlations were selected for use in this study.

Abou-el-Hassan (1983) has presented a generalized bubble rise velocity correlation based on dimensionless groups that account for the parameters affecting bubble rise velocity as well as bubble interaction. It is independent of flow regimes and is applicable for Reynolds numbers between 0.1 and 10^4. The correlation is in good agreement with literature data for air-bubble motion in Newtonian fluids and covers the following range of conditions:

liquid-phase density = 710 to 1180 kg/m^3

liquid-phase viscosity = 0.233 to 59 mPa.s

interfacial tension = 0.015 to 0.072 N/m

The correlation is given by:

$$V = 0.75\ [\log(F)]^2 \qquad \text{(V-15)}$$

where V (velocity number) and F (flow number) are defined as:

$$V = \frac{u_B d_B^{2/3} \rho_\ell^{2/3}}{\mu^{1/3} \sigma^{1/3}} \qquad \text{(V-16)}$$

$$F = \frac{g d_B^{8/3} (\rho_\ell - \rho_g) \rho_\ell^{2/3}}{\mu^{4/3} \sigma^{1/3}} \qquad \text{(V-17)}$$

The correlation is valid for velocity numbers in the range of 0.1 to 40 and flow numbers in the range of 1 to 10^6.

For bubble rise velocities greater than 0.15 m/s it was found that the correlation failed. Another correlation was used to determine the bubble

size for bubble rise velocities greater than 0.2 m/s (Clift et al., 1978),

$$u_B = \left[\frac{2.14\sigma}{\rho_f d_B} + 0.505 g d_b \right]^{1/2} \qquad (V\text{-}18)$$

The equation was developed from experimental data for air bubbles rising in distilled water, and is valid for bubble sizes greater than 1.3 mm.

For the range of bubble rise velocities not covered by the above two correlations, bubble diameters were obtained by interpolation. Figure V-65 shows the relation between rise velocity and bubble diameter for FT-300 wax at 265°C, with the interpolated values indicated by the broken line. These correlations can now be used to estimate d_{Bi} values using bubble rise velocities (u_{Bi}) obtained from the procedure outlined in the previous section.

The number of bubbles (n_i) of size d_{Bi} can be calculated as follows. The overall or average gas hold-up is given by:

$$\epsilon_{go} = \frac{V_g}{V_T} \qquad (V\text{-}19)$$

where V_g is the volume of gas in the gas-liquid dispersion and V_T is the expanded volume. Equation (V-19) can be rewritten as:

$$\epsilon_{go} = \sum_{i=1}^{N} n_i V_i / V_T \qquad (V\text{-}20)$$

where n_i is the number of bubbles of size d_{Bi} and V_i is the volume associated with this group of bubbles. Therefore, the hold-up associated with bubbles of size d_{Bi} can be expressed as:

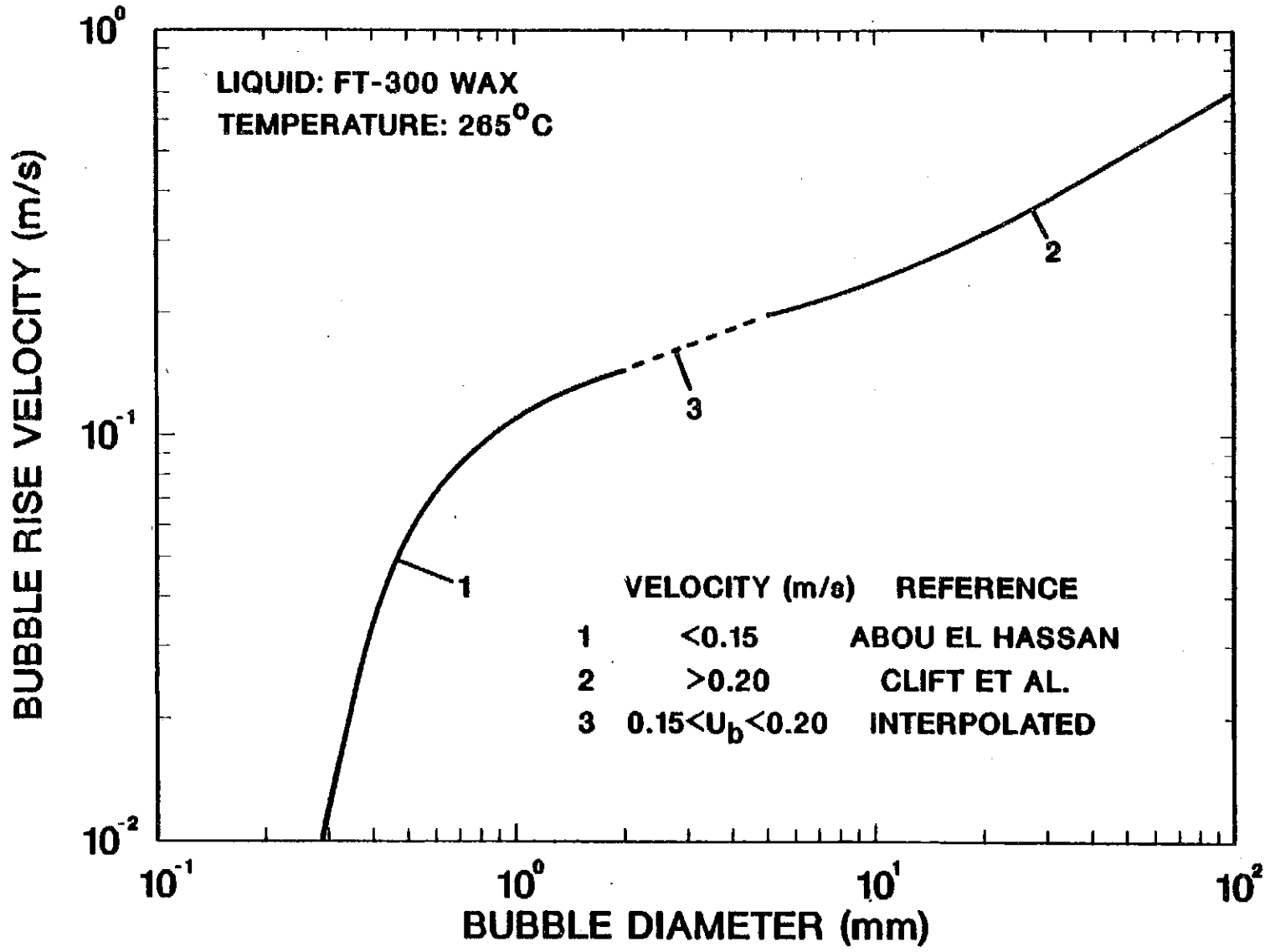

Figure V-65. Correlation of bubble rise velocity as a function of bubble diameter

$$\epsilon_{goi} = \frac{n_i V_i}{V_T} \tag{V-21}$$

or

$$n_i = \frac{\epsilon_{goi} V_T}{V_i} \tag{V-22}$$

The volume associated with bubbles of size d_{Bi} is given by:

$$V_i = \frac{\pi d_{Bi}^3}{6} \tag{V-23}$$

and the total volume is:

$$V_T = \frac{\pi d_c^2 H_c}{4} \tag{V-24}$$

where d_c is the column diameter. Substituting Equations (V-23) and (V-24) into Equation (V-22) yields:

$$n_i = \frac{3\epsilon_{goi} d_c^2 H_o}{2 d_{Bi}^3} \tag{V-25}$$

which may be used to calculate the number of bubbles of size d_{Bi}.

D.3a.4. Sauter Mean Diameter

By definition, the Sauter mean bubble diameter, d_s, is:

$$d_s = \frac{\sum_{i=1}^{N} n_i d_{Bi}^3}{\sum_{i=1}^{N} n_i d_{Bi}^2} \tag{V-26}$$

Substituting Equation (V-25) into Equation (V-26), yields upon rearrangement:

$$d_s = \frac{\sum_{i=1}^{N} \epsilon_{goi}}{\sum_{i=1}^{N} \epsilon_{goi}/d_{Bi}} \qquad \text{(V-27)}$$

D.3b. Experimental Procedure

A videocamera and a VCR unit were used to record the drop in liquid level during the disengagement process. A vertical ruler mounted next to the column (in the camera's field of view) was used to obtain the actual heights. After the completion of a run with a given gas velocity, the gas flow was shut off using a solenoid valve and the drop in liquid level recorded. The level dropped rapidly during the first 5 to 10 s after the gas flow was shut off, due to the disengagement of the large bubbles. Thereafter, the level dropped slowly as the medium size and small bubbles disengaged from the dispersion. The recording was completed when the level reached a stationary value (corresponding to the static height). Towards the end of the recording period, a large number of very tiny bubbles could be seen rising through the dispersion.

The data analysis procedure involved the analysis of the video tape followed by the data reduction procedure. The video tape was scanned and the time elapsed (t) recorded for different values of height (H) as the level dropped during the disengagement process. The data were recorded directly into a personal computer. The frequency at which time was recorded ranged from every 0.05 m drop in level (during the initial period when the level dropped rapidly) to every 0.005 m drop in level (towards the end when tiny bubbles were disengaging). This procedure was repeated three to four times for each velocity to reduce errors. Following this step, the normalized liquid level (H/H_o) plot was directly displayed on the screen.

Appropriate break points were then selected by the user and plots similar to those shown in Figure C-1 (APPENDIX C) obtained. The slopes and intercepts of the straight line segments were then computed and the corresponding rise velocities and hold-up fractions obtained. The computer then calculated bubble sizes for each class of bubbles, the number of bubbles in each class and finally the Sauter mean diameter. A summary data sheet for every run, similar to those shown in APPENDIX D, was then printed out.

D.3c. Experimental Results

DGD measurements were made after a minimum of one and a half hour per velocity for velocities between 0.01 and 0.05 m/s, and a minimum of 1 hour for velocities greater than 0.05 m/s except for a few runs as discussed below. It was necessary to wait for this duration to ensure that steady state was achieved, particularly when foam was present. Summary of results for selected runs are included in APPENDIX D.

D.3c.1. Effect of Operating Temperature

Figure V-66a is a plot of the Sauter mean bubble diameter (d_s) as a function of superficial gas velocity for experiments conducted with FT-300 wax in the 0.051 m ID column using a 1.85 mm orifice plate distributor. Average gas hold-up values for these runs are shown in Figure V-66b. Figures V-68a and V-68b show similar results for runs conducted with Sasol's Arge wax.

Sauter mean diameter values for FT-300 wax at 265°C (Figure V-66a) are consistently lower than values at 200°C for all velocities, except at 0.01 m/s. In the presence of foam (u_g = 0.02 to 0.05 m/s), d_s at 200°C is 50% higher than d_s at 265°C (0.75 mm compared to around 0.5 mm). This